CHAPTER IV

RESULTS AND DISCUSSION

In this research, novel pyrrolidinyl PNAs carrying 3-aminopyrrolidine-4-carboxylic acid (APC) spacer were synthesized. The structure of APC spacers were designed based on our previously reported PNA system bearing (1*S*,2*S*)-2-aminocyclopentane carboxylic acid (ACPC) spacer (a), with additional nitrogen atom in the cyclopentane ring of the *β*-amino acid. The general structures of *acpc*PNA and *apc*PNA were as shown in Figure 24.

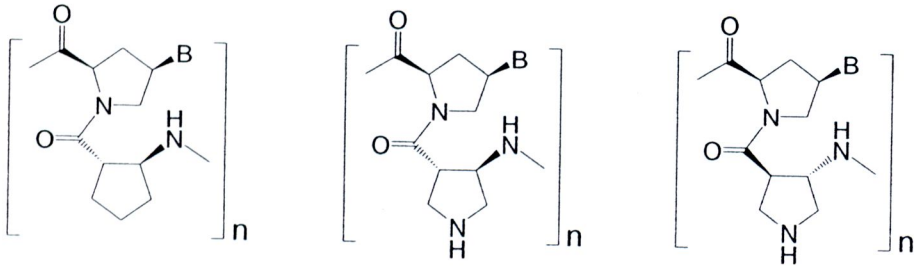

Figure 24 (a) *acpc*PNA, (b) *(3R,4S)-apc*PNA and (c) *(3S,4R)-apc*PNA

The synthesis of PNA oligomer was separated into two parts. The first part involves synthesis of the *β*-amino acid monomer; 3-aminopyrrolidine-4-carboxylic acid (APC) spacers. The second part is synthesis of the PNA oligomer *via* solid phase peptide synthesis.

Synthesis of 3-aminopyrrolidine-4-carboxylic acid (APC) spacer

Synthesis of *trans*-(3*R*,4*S*) and *trans*-(3*S*,4*R*) isomer of 3-aminopyrrolidine-4-carboxylic acid spacers was previously reported by Rapoport [43] and Gellman [44]. The synthesis route described by Gellman started from Diekmann cyclization of Boc-glycine ethyl ester with ethyl acrylate to give *β*-keto-ester. Diastereoselective reductive amination of the *β*-keto-ester with (*S*)- or (*R*)-α-methylbenzylamine

followed by protecting group exchange gave the (3*R*,4*S*)- or (3*S*,4*R*)-isomers as the protected spacers in 6.5% and 4.9% overall yield, respectively. The synthetic scheme of (3*R*,4*S*)-isomer was shown in Figure 25 and (3*S*,4*R*)-isomer used (*R*)-(+)-α-methylbenzylamine instead of (*S*)-(−)-α-methylbenzylamine in same manner.

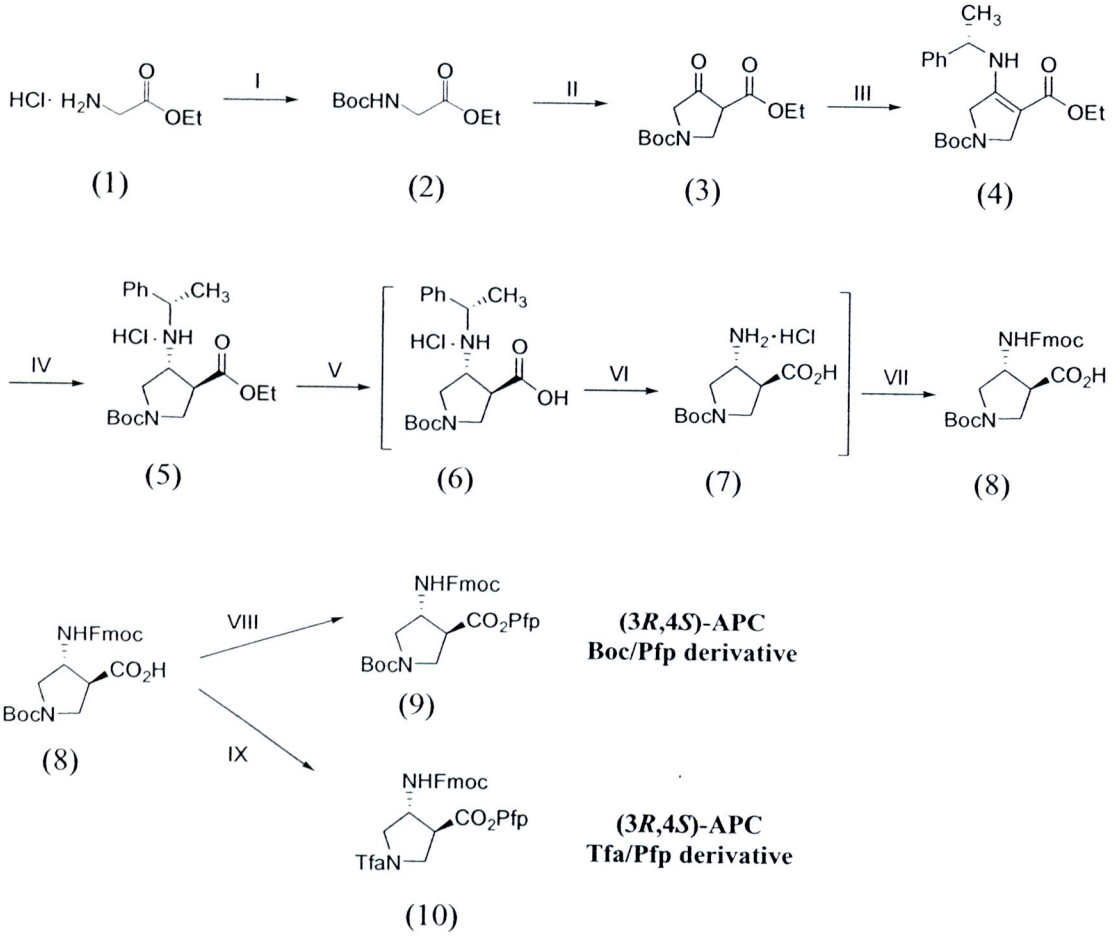

Reagent and Condition: (I) Boc_2O, Et_3N, MeOH 30°C (II) ethyl acrylate, KO^tBu, toluene, 0°C, N_2 (III) (*S*)-(−)-methylbenzylamine, AcOH, EtOH, rt (IV) $NaBH_3CN$, 75°C and 4 N HCl in EtOAc 0°C (V) $LiOH·H_2O$, $THF/CH_3OH/H_2O$, 0°C (VI) H_2, 10% Pd/C, 95% EtOH (VII) Fmoc-OSu, $NaHCO_3$, $acetone/H_2O$ 0°C to rt (VIII) PfpOH, DIEA, CH_2Cl_2 (XI) 1) TFA in CH_2Cl_2 2) PfpOH, DIEA, CH_2Cl_2.

Figure 25 The synthetic scheme of (3*R*) -aminopyrrolidine-(4*S*)-carboxylic acid derivative [43, 44]

The commercially available glycine ethyl ester hydrochloride was used as the starting material for APC spacers by protecting with the *tert*-butoxycarbonyl (Boc) group at the highly nucleoplilic sites of the compound (NH) in the first step. The reaction of glycine ethyl ester hydrochloride (**1**) and di-*tert*-butyl dicarbonate (Boc_2O) in methanol using triethylamine as base to gave carbon dioxide and *tert*-butanol as by-product. The identity of Boc-glycine ethyl ester (**2**) was confirmed by ^1H NMR, which shows a triplet peak at 4.08 ppm due to $C\underline{H}_3$ of the ethyl group, a quartet peak at 1.25 ppm due to $C\underline{H}_2$ of the ethyl group, a doublet peak at 3.552 due to $C\underline{H}_2$ of the α-carbon and one sharp singlet peak at 1.43 ppm of the Boc group.

After the Boc-glycine ethyl ester was obtained, the compound **2** was reacted with ethyl acrylate and potassium *t*-butoxide (KO^tBu) at 0 °C to give ethyl 1-*tert*-butoxycarbonyl-3-oxopyrrolidine-4-carboxylate (**3**). The mechanism of this reaction was divided into two steps. The first step was an 1,4-addition reaction from the nitrogen nucleophile of compound **2** attack at a double bond terminal site of ethyl acrylate to give the intermediate N. In the next step, the intermediate N was deprotonated by KO^tBu at α-carbon that have two position near the carbonyl group to give enolate anion followed by the intramolecular substitution reaction on Diekmann cyclization type to give the five-membered ring as the β-keto-ester (**3** and **3-A**) (Figure 26). A proton at α-carbon of glycine (acetic methylene proton; pK_a = 3.66) is acidic more than the proton at α-carbon of ethyl acrylate (propionic methylene proton pK_a = 4.76) because the inductive effect of *N*-Boc group which is consistent with the results of Rapoport reported that to give compound **3** than compound **3-A** [43]. The compound **3** and **3-A** can isolated by extraction with carbonate buffer pH 9.5 that the half life of compound **3** is 10 days in this solution while the compound **3-A** has 2 minus of a half-life [43]. The extracts were purified by column chromatography to give the β-keto-ester as compound **3** in 66% yield.

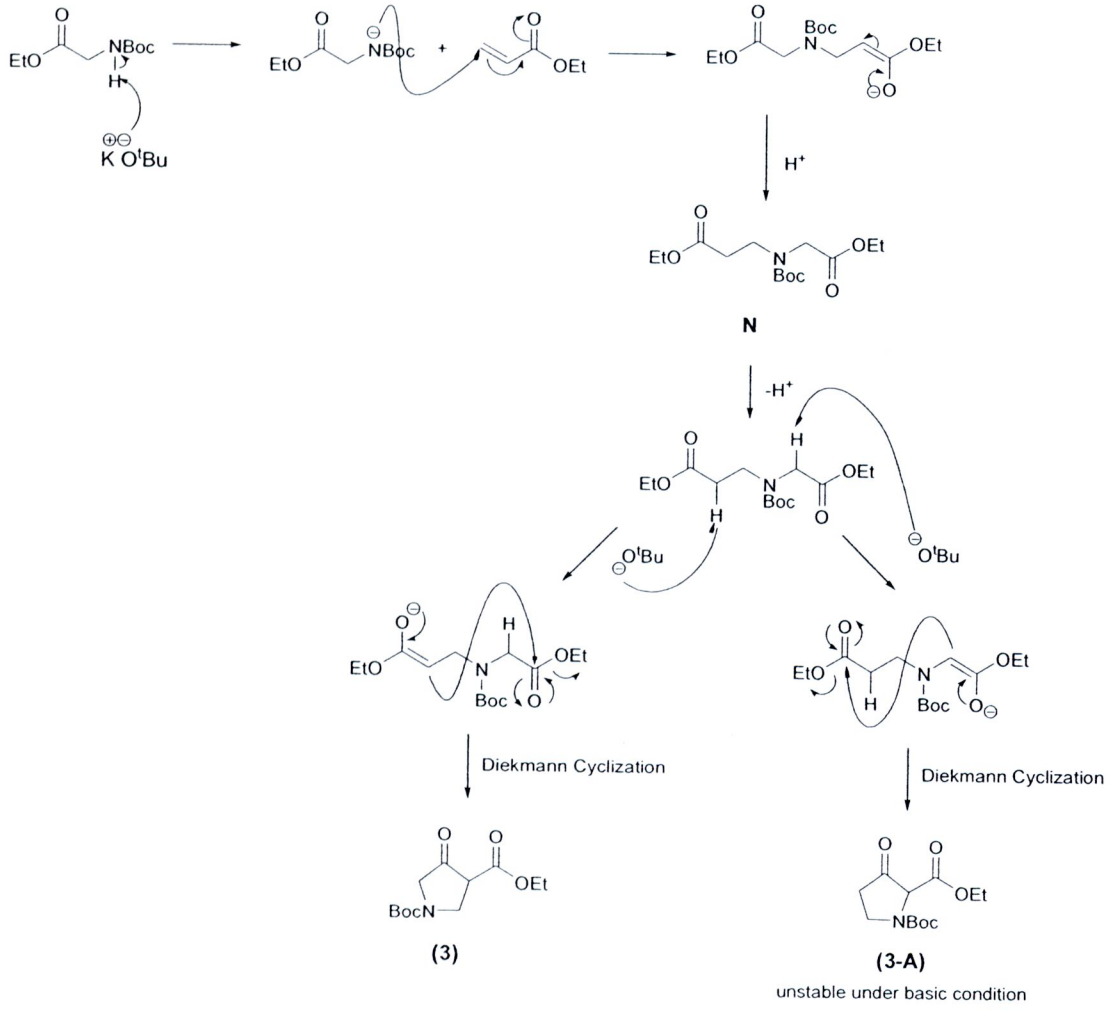

Figure 26 Mechanism of Diekmann cyclization of Boc-glycine ethyl ester (2) to give ethyl 1-*tert*-butoxycarbonyl-3-oxopyrrolidine-4-carboxylate (3)

The *β*-keto-ester **3** was reacted with (*S*)-(−)-α-methylbenzylamine in the presence of glacial acetic acid to give the enamine intermediate **4**. The enamine was stereoselectively reduced with sodium cyanoborohydride to give the (3*R*,4*S*)-*trans* isomer (**4**) along with other stereoisomers. The desired diastereomer could be separated the crystalline HCl salt by treatment with 4 N HCl in ethyl acetate followed by recrystallization from acetonitrile to give compound **5** in 21% yield. The structure was confirmed by comparison of ^{1}H NMR spectrum and the specific rotation value ($[\alpha_D^{27}]$ = –4.6, c = 1.00 in MeOH). The enantiomeric (3*S*,4*R*)-APC isomer (**12**) was prepared by reacting with (*R*)-(+)-α-methyl-benzylamine. The specific rotation value

($[\alpha_D^{27}]$ = +4.6, c = 1.00 in MeOH) was compared with the value reported in the literature ($[\alpha_D^{23}]$ = +4.8, c = 1.05 in MeOH). The compound 5 was hydrolyzing with the lithium salt and treatment with dilute acid to generate the free carboxylic acid (**6**). The (*S*)-methylbenzylamine chiral auxiliary was removed from compound **6** by hydrogenation over palladium hydroxide on charcoal catalyst to give the free amino acid (**7**). The free amino group was further protected with Fmoc group by reacting with 9-fluorenylmethyl succinimidyl carbonate (FmocOSu) under basic condition and purified by crystallization from *n*-heptane/ethyl acetate to afford the Fmoc-(3*R*)-aminopyrrolidine-(4*S*)-carboxylic acid (**8**) in 78% yield (from compound **5**). The correct stereoisomer was confirmed by optical rotation. The specific rotation value of compound **8** ($[\alpha_D^{27}]$ = +21.88, c = 1.00 in MeOH) was compared with the value reported in the literature [44] ($[\alpha_D^{23}]$ = +18.30, c = 1.20 in MeOH). The condensation reaction between a carboxylic acid and an amine to from amide bond requires activation of the carbonyl group, so the Fmoc protected acid (**8**) was also activated with Pfp group by reacting with PfpOTfa/DIEA. The Fmoc/Pfp APC monomer (**9**) was obtained as a white solid in 60% yield.

In order to attach of pyrene fluorescence label on *apc/acpc*PNAs, the APC spacers will need to be protected with trifluoroacetyl (Tfa) group at the nitrogen atom on APC pyrrolidine ring to be compatible with the Fmoc SPPS because in deprotection step for attach the pyrene fluorescence label, the Boc group can be deprotected by TFA that can be cleaved the amino linker between the PNA and resin but the trifluoroacetyl group on APC spacer will not be cleaved for deprotected with NH_3/dioxane. The compound **8** was treated with trifluoroacetic acid (TFA) to remove the Boc group and simultaneously protected with Tfa group and activated with Pfp group by reacting with PfpOTfa/DIEA to give the compound **10** in 60% yield.

Synthesis of *apc*PNA oligomers

In this research, Fmoc-based solid phase peptide synthesis [47] was employed to construct the *apc/acpc*PNA. The desired PNA sequence was obtained by alternately coupling of the Fmoc-protected PNA monomer and APC spacer or ACPC spacer onto a solid support according to the previously developed protocol [45]. The microscale synthesis of PNA was carried out manually from Fmoc-protected monomers in a

custom-made Pasteur pipette as described in **Chapter III**. The TentaGel S RAM [48] resin containing a polyethylene glycol (PEG) grafting on polystyrene resin and a moderately acid labile Rink amide (RAM) linker [49] (Figure 27) was used as the solid support for all PNA syntheses. This linker is stable to piperidine, which is used in Fmoc deprotection, and can be easily cleaved with 95-100% TFA to provide peptide amides. Furthermore, the amino linker of RAM resin allows easy coupling with active esters such as pentafluorophenyl (Pfp) ester to form amide bonds.

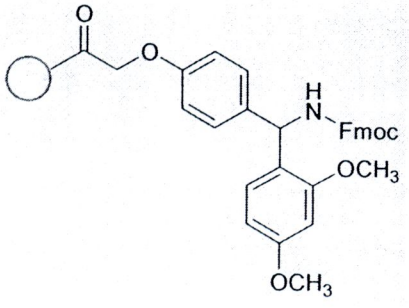

Figure 27 TantaGel S RAM Fmoc resin

The TentaGel resin containing a polystyrene matrix with a PEG modifier was chosen as the support for PNA synthesis because it is swellable in many solvent, especially in dimethylformamide (DMF) which is the only solvent used for Fmoc-SPPS in this study. The swelling property of the solid support will determine how the reactant can access reactive sites on the solid support which has a direct consequence on the synthesis efficiency.

Synthesis of PNA (**P2**) consists of three important steps. These include i) deprotection step, the Fmoc group protected amino was removing by using 20% piperidine in DMF to give free amino. ii) coupling step, the monomer or spacer was alternately coupled until to give the required sequence. iii) capping step, the resin-bond amino group that had not been successfully coupled was capped by an acetyl group for stopping incomplete reaction in the next cycle. After end-capping by acetylation or benzoylation, the nucleobase side chain protecting groups was removed by treatment with 1:1 aqueous ammonia/dioxane at 60 °C overnight. This condition also simultaneously removed the *N*-Tfa protecting group on the Tfa-protected APC

unit. Several fluorescent labels including pyrenecarboxylic acid (Py) and pyrene-butyric acid (PyBu) were successfully incorporated. These were usually coupled directly to the nitrogen atom of APC spacer of the PNA using HATU/DIEA as activators. The synthesis cycle of SPPS originally used in this study is exactly as described in the literature [45]. The details synthesis cycle of PNA used in this work is shown in Figure 23.

The successfully synthesized PNA were purified by C-18 reverse-phase HPLC with UV detection at 260 nm and characterized by MALDI-TOF mass spectrometry which showed the expected mass of the molecular ion $[M+H]^+$ or $[M]^+$ as shown in Table 4. Typical examples of HPLC chromatogram and mass spectrum of PNA **P2** are illustrated in Figure 28. Fractions containing the pure PNA were combined and freeze-dried. The residues were re-dissolved in 150 μL of water and the concentration of the PNA was determined by spectrophotometrically. The yield of PNA can be monitored by concentration measurement of the absorbance at 260 nm of purified PNA oligomers as shown in Table 3.

Table 3 Yield of PNA sequences in this study.

	PNA[a]	Scale (μmol)	Percent yield (%)
P2	Bz-$\underline{\text{TTTTTTTT}}$-Lys-$NH_2$	1.5	7.1
P3	Bz-$\underline{\underline{\text{TTTTTTTT}}}$-Lys-$NH_2$	1.5	8.7
P4	Bz-TTTT$\underline{\text{T}}$TTTT-Lys-NH_2	2.0 (split in to 2 reaction)	10.1
P5	Bz-TTTT$\underline{\underline{\text{T}}}$TTTT-Lys-$NH_2$		16.2
P6	Bz-GTAGA$\underline{\text{T}}$CAC T-Lys-NH_2	1.5	4.5
P7	Ac-TTTT$^{(\text{Py})}\underline{\text{T}}$TTTT-Lys-$NH_2$	2.0 (split in to 2 reaction)	2.3
P8	Ac-TTTT$^{(\text{PyBu})}\underline{\text{T}}$TTTT-Lys-$NH_2$		8.7
P9	Ac-GTAGA$^{(\text{Py})}\underline{\text{T}}$CAC T-Lys-$NH_2$	1.5	5.5
P10	Bz-GTAGA$^{(\text{PyBu})}\underline{\text{T}}$CAC T-Lys-$NH_2$	1.5	2.4

[a] T = (1*S*,1*S*)-ACPC-T; G = (1*S*,1*S*)-ACPC-G; C = (1*S*,1*S*)-ACPC-C; A = (1*S*,1*S*)-ACPC-A; $\underline{\text{T}}$ = (3*R*,4*S*)-APC-T; $\underline{\underline{\text{T}}}$ = (3*S*,4*R*)-APC-T

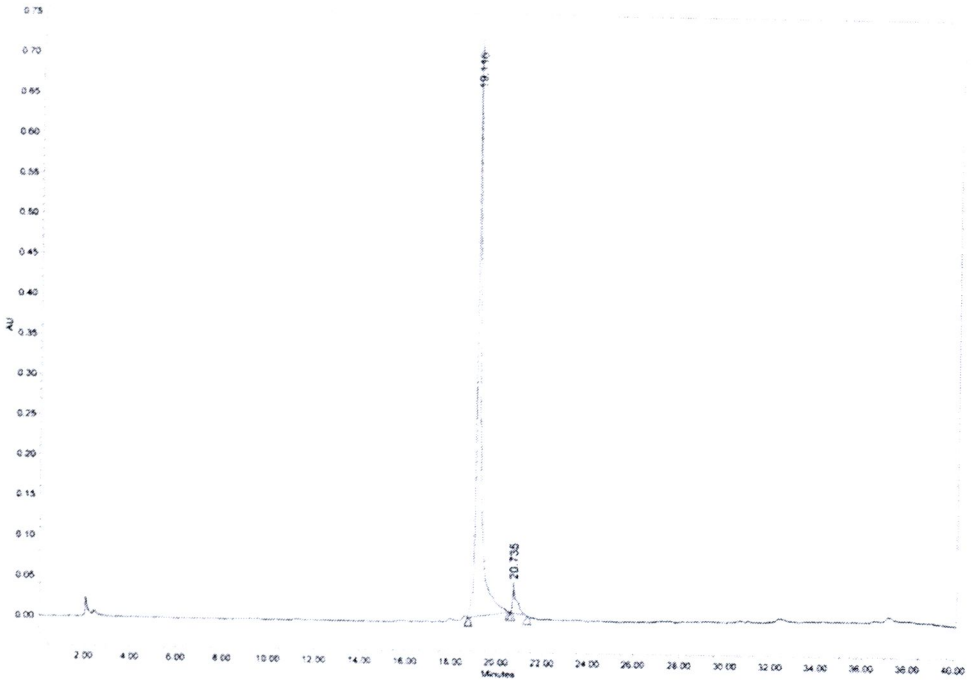

(a)

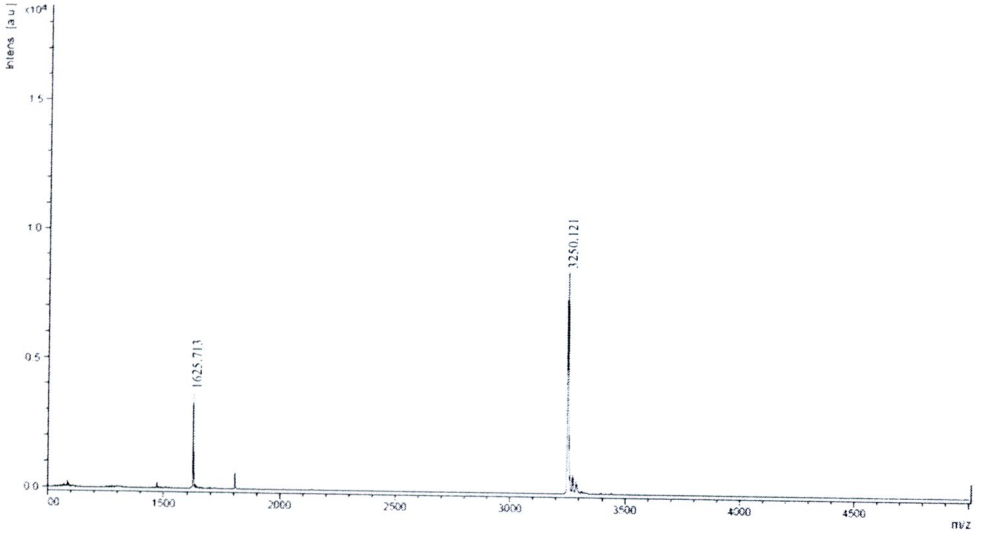

(b)

Figure 28 (a) HPLC chromatogram of purified PNA (P2) and (b) MALDI-TOF MS of purified PNA (P2)

Table 4 Characterization data of PNA sequences.

	PNA[a]	t_R[b]	M·H$^+$ (found)	M·H$^+$ (calcd)
P2	Bz-$\underline{\text{TTTTTTTT}}$-Lys-$NH_2$	19.1	3250.5	3250.1
P3	Bz-$\underline{\underline{\text{TTTTTTTT}}}$-Lys-$NH_2$	18.6	3250.5	3251.2
P4	Bz-TTTT$\underline{\text{T}}$TTTT-Lys-NH_2	22.2	3242.5	3242.6
P5	Bz-TTTT$\underline{\underline{\text{T}}}$TTTT-Lys-$NH_2$	22.3	3242.5	3243.7
P6	Bz-GTAGA$\underline{\text{T}}$CACT-Lys-NH_2	20.6	3621.9	3622.2
P7	Ac-TTTT$^{(\text{Py})}\underline{\text{T}}$TTTT-Lys-$NH_2$	23.7	3409.6	3411.0
P8	Ac-TTTT$^{(\text{PyBu})}\underline{\text{T}}$TTTT-Lys-$NH_2$	24.8	3452.0	3451.6
P9	Ac-GTAGA$^{(\text{Py})}\underline{\text{T}}$CACT-Lys-$NH_2$	21.3	3788.9	3789.4
P10	Bz-GTAGA$^{(\text{PyBu})}\underline{\text{T}}$CACT-Lys-$NH_2$	22.7	3893.0	3893.7

[a] T = (1*S*,2*S*)-ACPC-T; G = (1*S*,2*S*)-ACPC-G; C = (1*S*,2*S*)-ACPC-C; A = (1*S*,2*S*)-ACPC-A; $\underline{\text{T}}$ = (3*R*,4*S*)-APC-T; $\underline{\underline{\text{T}}}$ = (3*S*,4*R*)-APC-T, (Py) = pyrene-1-carbonyl modification; (PyBu) = 4-(pyrene-1-yl)butyryl modification

[b] Condition for reverse-phase HPLC: C-18 column 3μ particle size 4.6 x 50 mm; gradient system of 0.01% TFA in acetonitrile/water 10:90 to 90:10 in 25 min; flow rate 0.5 mL/min.

Hybridization of *apc/acpc*PNA with DNA

Thermal denaturation or melting temperature (T_m) measurement was the principal technique for determining the binding property and sequence specificity of PNA·DNA hybrids. PNA·DNA denaturation refers to the melting of double stranded DNA to generate two single strands at high temperature. This involves the breaking of hydrogen bonds between the bases in the duplex that are stabilized by additional hydrophobic, π-π and dipole-dipole interaction between the stacked base pairs. In general, the resulting of base-base stacking provides the decrease the molar extinction coefficient (ε) value which in known as hypochromism [50]. The hypochromism can be observed in DNA·DNA duplex as well as PNA·DNA complex. Dissociation of the duplex into single stranded oligonucleotides, e.g. by heating resulted in unstacking of the DNA or PNA base which was accompanied by a slight increase in the extinction coefficient (~10-20%) (hyperchromism). The hyperchromicity is conveniently monitored at 260 nm, the wave length at which all four nucleobases strongly absorb.

The resulting plot is known as "melting curve" which is S-shaped (Figure 29). The temperature at the midpoint of the melting curve is known as melting temperature (T_m) which corresponds to a temperature at which 50% of duplex has been dissociated. This value provides information on the stability of the duplex structure. Stable duplexes melt at a higher melting temperature than less stable duplexes. The cooperativity between base-base interactions required that the melting process occurs abruptly within only 10-20 °C range. Once the input energy is sufficient to break the first hydrogen-bonded base pair, the dissociation continues until the two strands completely separate. From the melting curve, the melting temperature (T_m) could be determined from the maxima of the first derivative plot (dA/dT) against temperature as shown in Figure 30.

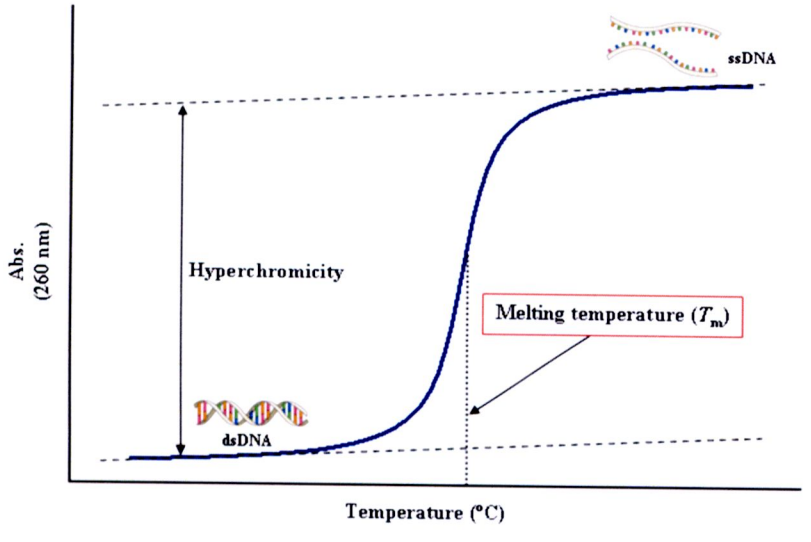

Figure 29 The change of UV absorbance in a typical thermal denaturation experiment of DNA duplex

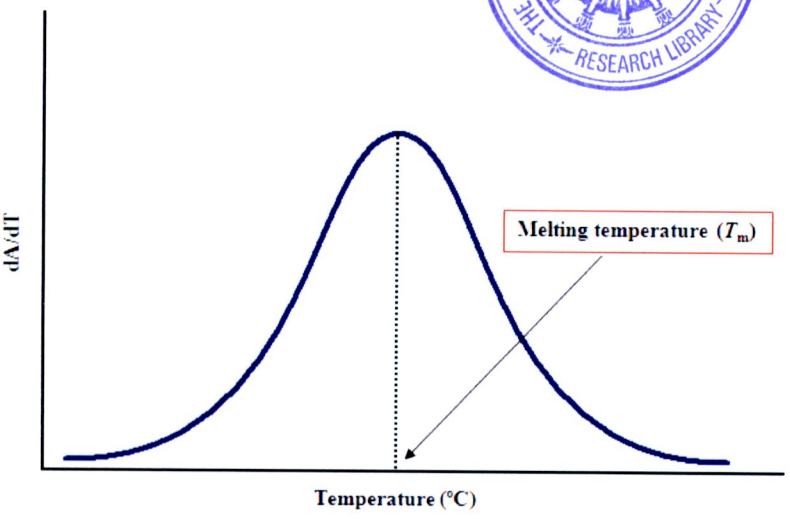

Figure 30 The first derivative plot obtained from a typical thermal denaturation experiment of DNA duplex

In a preliminary experiment, the melting temperatures (T_m) of *apc*/*acpc*PNA **(P2-P6)** hybrid with complementary DNA were measured as shown in Figure 31.

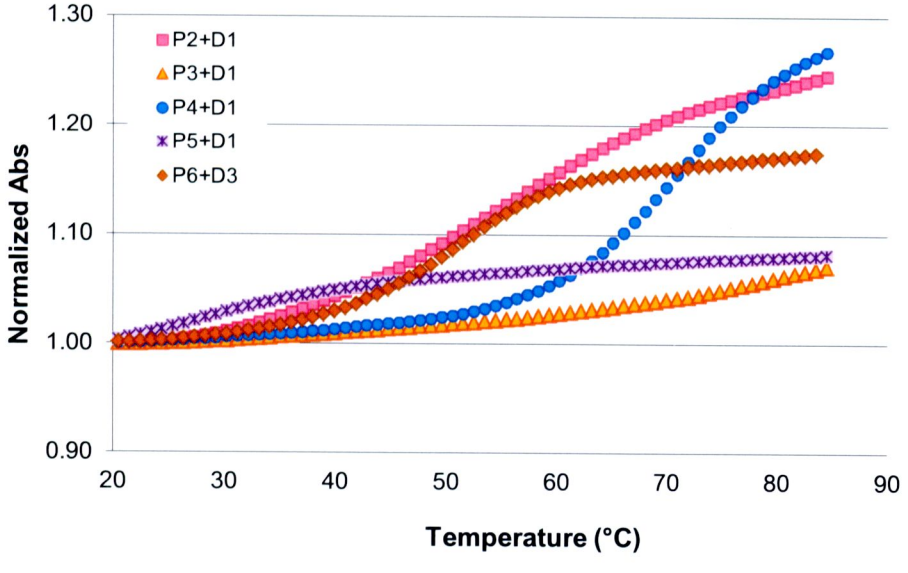

Figure 31 T_m curves of PNA (P2-6) hybrid with complementary DNA Condition: 10 mM sodium phosphate buffer pH 7.0, 100 mM NaCl, [PNA] = 1.0 μM and [DNA] = 1.0 μM

The results of T_m experiments of hybrids between PNA (**P1-P6**) and their complementary and single mismatched DNAs are summarized in Table 5.

Table 5 T_m data of PNA (P1-P6) oligomers in this study

PNA	DNA sequence (5'→3')		Note	T_m (°C) [a]	Δ T_m (°C) [b]
P1	**D1**	AAAAAAAAA	perfect match	75.6	-
P2	**D1**	AAAAAAAAA	perfect match	55.5	-
	D2	AAAAT̲AAAA	single mismatch	nd	-
P3	**D1**	AAAAAAAAA	perfect match	<20	-
	D2	AAAAT̲AAAA	single mismatch	-	-
P4	**D1**	AAAAAAAAA	perfect match	71.1	-
	D2	AAAAT̲AAAA	single mismatch	43.1	28.0
P5	**D1**	AAAAAAAAA	perfect match	28.3	-
P6	**D3**	AGTGATCTAC	perfect match	50.8	-
	D4	AGTGAC̲CTAC	single mismatch	29.5	21.3

[a] nd = not detected, Condition: **P1-P6** = 10 mM sodium phosphate buffer pH 7.0, 100 mM NaCl, [PNA] = 1.0 μM and [DNA] = 1.0 μM

[b] $\Delta T_m = T_m$(complementary) – T_m(mismatched) (same PNA, different DNA)

The results of T_m data demonstrated that each PNA oligomer can hybridize with its complementary DNA target in different stabilities. Upon heating a 1:1 mixture of the homothymine nonamer PNA (**P2**) and its complementary DNA (**D1**), a typical sigmoidal melting curve was observed, as was evident from the sharp increase in the absorbance at 260 nm. The single-stranded PNA or DNA showed no such melting behavior in the absence of the DNA complementary strand. This suggests that the *apc*-modified PNA can form a hybrid with DNA. The T_m value of a T_9 PNA **P2** and **P3** with dA_9 (**D1**) was estimated to be 55.5 °C and <20 °C compared with original **P1**. The results showed that the fully modified of (3*R*,4*S*)-APC spacer in the pyrrolidine PNA system moderately decrease the DNA binding stability (ΔT_m (modified – unmodified) = –20.1 °C). However, the (3*R*,4*S*)-*apc*PNA·DNA duplex stability was still high when compared with DNA·DNA duplex (T_m = 21 °C) [51]. The singly modified **P4** carrying

(3*R*,4*S*)-APC spacer which possess the same absolute configuration as (1*S*,2*S*)-ACPC could bind with complementary DNA in high T_m (71.1 °C) compared with PNA **P1** (ΔT_m (modified – unmodified) = –4.5 °C), the T_m only slightly lower than unmodified *acpc*PNA. The T_m value of singly modified **P5** carrying (3*S*,4*R*)-APC spacer with complementary DNA was only 28.3 °C. The results of T_m data showed that the singly modified of **P4** carrying (3*R*,4*S*)-APC can bind with complementary DNA and give high T_m similar to the unmodified *acpc*PNA **P1.** In contrast, the singly modified with (3*S*,4*R*)-APC spacer of **P5** showed expectedly a dramatic decreased in T_m because (3*R*,4*S*)-APC spacer has possess the same absolute configuration as (1*S*,2*S*)-*acpc*PNA. For mixed base sequences, the PNA **P6** showed a normal melting behavior to *acpc*PNA (T_m = 58 °C) [45] with slightly decreased T_m (ΔT_m (modified – unmodified) = –7.2 °C). The presence of a single mismatch base in the DNA strand resulted in lowering of the T_m value of the complex by 21-28 °C, indicating that the specificity remains high.

The stoichiometry of the PNA·DNA complex was determined by UV titration experiment [52]. In these experiments, the T_9 PNA was added to the DNA solution phosphate buffered (10 mM, pH 7.0) in several aliquots and the UV absorbance at 260 nm was measured after each addition. A significant deviation of the observed UV absorbance at 260 nm from the calculated value due to hypochroism was observed when dA_9 as analyst was titrated with T_9 of **P2**, **P3** and **P4** (Figure 29). The ratio of observed and calculated value at 260 nm was plotted against percent mole fraction of PNA. The UV-titration data showed interesting manner of PNA; the **P4** which was singly modified with (3*R*,4*S*)-APC spacer showed an inflection point around 50% of DNA, which indicated the formation of 1:1 PNA·DNA complex. This 1:1 stoichiometry is resemble to *acpc*PNAs. The fully modified **P2** showed an inflection point around 35% of DNA, suggesting a 2:1 PNA:DNA ratio. The possible explanation of this behavior is that **P2** can be protonated at the nitrogen atom of the APC spacer throughout the sequence. This makes that the second strand and third strand of PNA became positively charged which can strongly bind with negatively charges DNA target. The electrostatic interactions between positively changed of third strand and negatively charged of DNA lead to 2:1 PNA-DNA hybrid. PNA **P3** did not show any equivalent point as expected because of the wrong configuration of spacer.

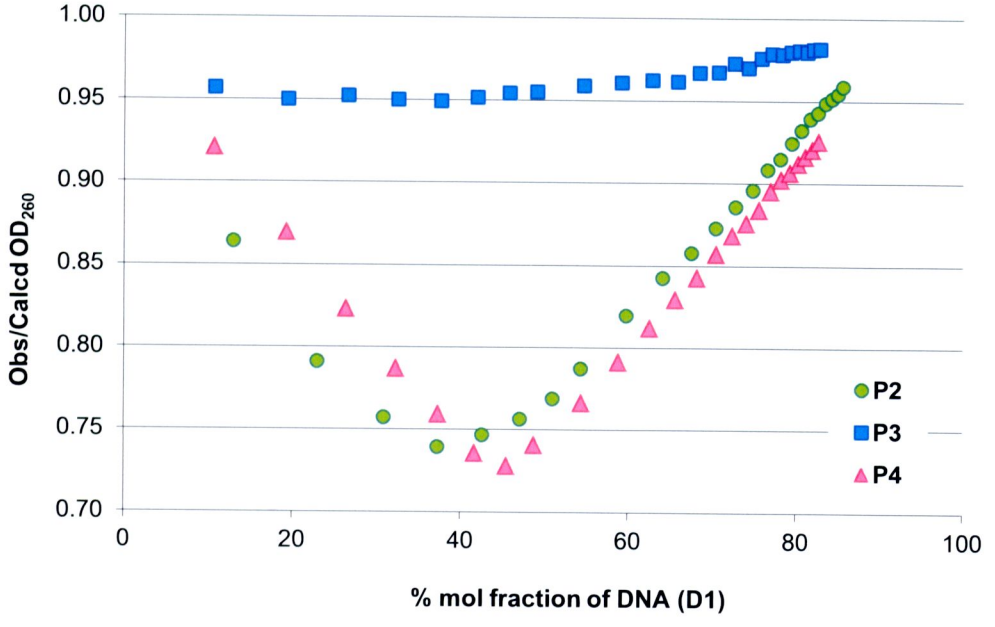

Figure 32 UV titration plot of DNA (D1) and T_9 PNA (P2, P3 and P4) Condition: 10 mM sodium phosphate buffer pH 7.0, 100 mM NaCl and [PNA] = 2.0 μM

Cirular dichroism spectroscopy (CD) which is a powerful technique used to establish the interaction of nucleic acids was also used for studying the interaction of PNA and DNA [53]. If hybridization with DNA occurs, an induced CD signal should be observed especially where the nucleobase chromosphores absorb, i.e. 250-280 nm, due to the bases becoming re-oriented as they from the stack [54]. The 1:1 mixture of T_9 (**P2**) with dA_9 showed a significantly different CD spectrum from the calculated sum of the CD spectra of individual components. This clearly indicates the conformational change induced by PNA·DNA hybridization. The stoichiometry was also studied by circular dichroism (CD) experiment. The CD spectra of the same T_9 PNA and dA_9 mixture at different ratio were measured. The CD signal of 2:1 hybrid formed between PNA **P2** and DNA **D1** showed negative bands at 208, 248 and 266 nm and positive bands at 219, 258 and 286 nm (Figure 33) compared to the *acpc*PNA that it forms a triplex with DNA in addition to the duplex. This is in good agreement with the UV titration experiment above. The CD spectra of **P3** and **P4** showed signal of 1:1 hybrid formed which are similar to those of the duplex formed between *acpc*PNA and dA_9 as shown in Figure 34 and Figure 35.

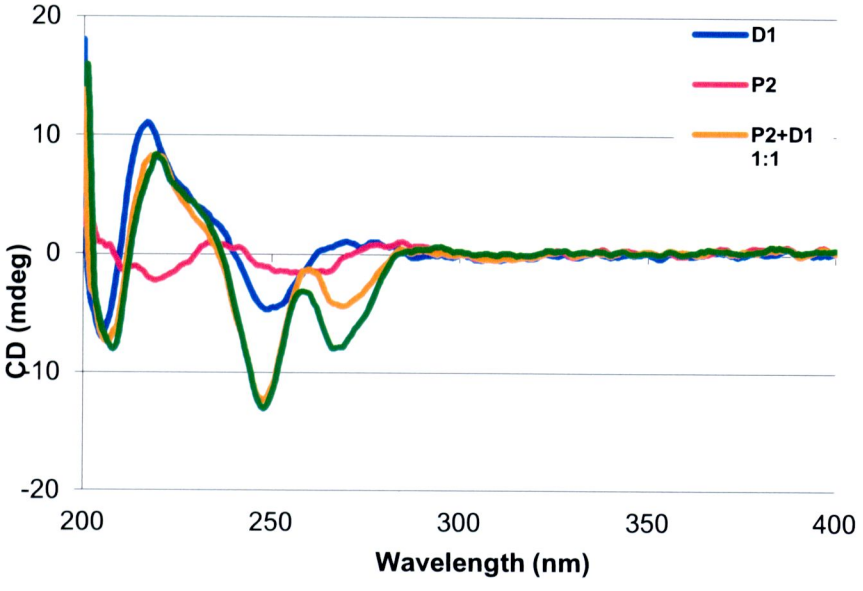

Figure 33 CD titration spectra of DNA (D1) and T_9 PNA (P2) Condition: 10 mM sodium phosphate buffer pH 7.0, 100 mM sodium chloride, [PNA] = 2.5 μM and [DNA] = 3.0 μM

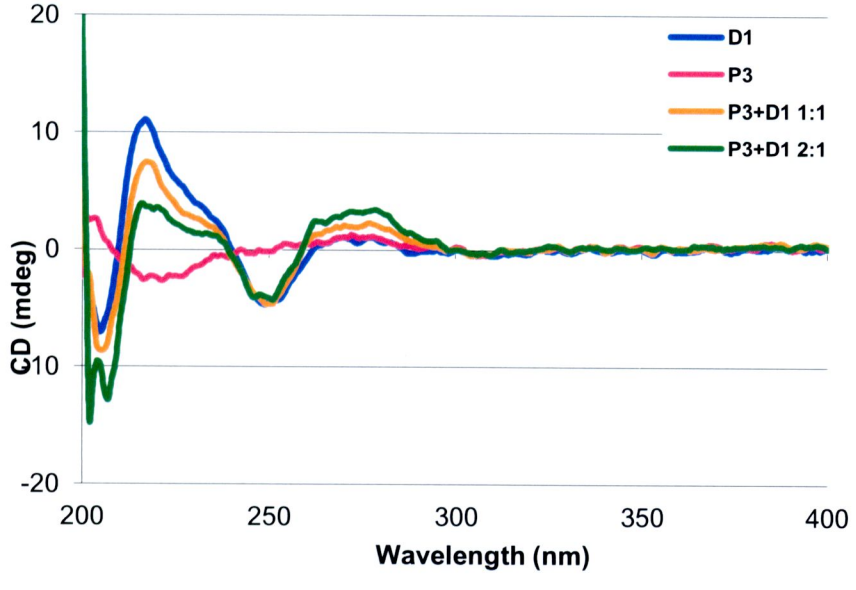

Figure 34 CD titration spectra of DNA (D1) and T_9 PNA (P3) Condition: 10 mM sodium phosphate buffer pH 7.0, 100 mM sodium chloride, [PNA] = 2.5 μM and [DNA] = 3.0 μM

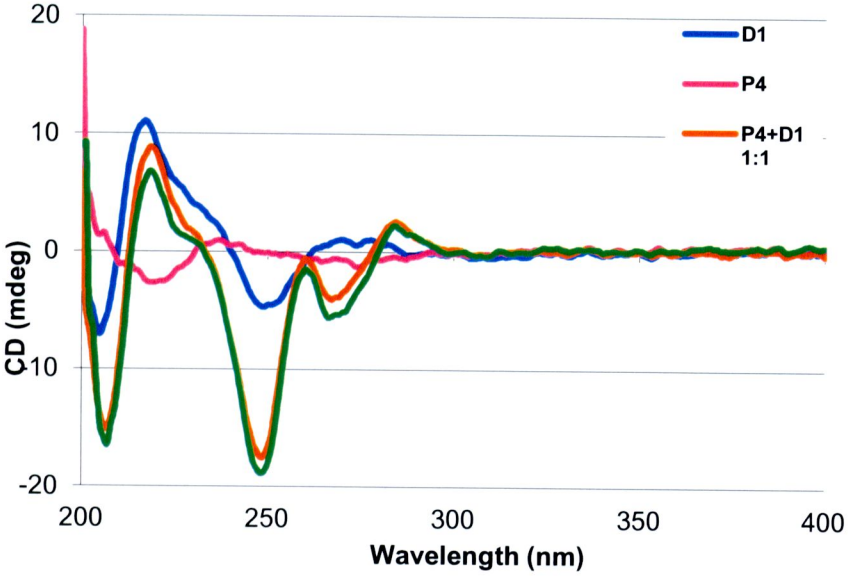

Figure 35 CD titration spectra of DNA (D1) and T_9 PNA (P4) Condition: 10 mM sodium phosphate buffer pH 7.0, 100 mM sodium chloride, [PNA] = 2.5 μM and [DNA] = 3.0 μM

The effect of pH to PNA·DNA hybridization was also investigated. The T_m value of PNA **P2** at pH 6 and 7 is lower than the T_m value under higher pH condition (pH 8). Furthermore, the sharp of T_m curve at pH 6 is similar to the curve at pH 7.0 whereas T_m curve is more sharpening of the T_m curve at pH 8 (Figure 36 and Table 6). This might be explained in terms of protonation of the pyrrolidine nitrogen (pK_a~8.75) [55] at low pH to form a positively charged side-chain which can interact electrostatically with the negatively-charged phosphate backbone of the DNA that PNA **P2** can bind with complementary DNA in the triplex formation. At higher pH, the nitrogen atom would become less protonated, hence the electrostatic attraction should decrease. The behavior of the APC spacer at high pH would therefore be more closely resemble that of the non-ionizable ACPC spacer which showed higher T_m value and more sharpening of the T_m curve. On the other hand, the singly-modified PNA (**P4**) formed only duplex with complementary DNA that electrostatic effect is much less in the PNA **P4** which was singly modified in the middle of the strand with APC spacer (Figure 37 and Table 6). The triplex formation should not be a problem because for labeling purpose the PNA would need to be modified with only one or up

to a few APC residues. Furthermore, upon modification by the amide bond formation, the APC residue should no longer be protonated at neutral pH.

Table 6 T_m data of DNA (D1) with PNA (P2, P4) hybrid at pH 6.0-8.0.

PNA	DNA sequence (5'→3')	pH	T_m (°C) [a]
P2	(D1) AAAAAAAAA	6.0	55.2
		7.0	55.5
		8.0	59.3
P4	(D1) AAAAAAAAA	6.0	68.8
		7.0	71.1
		8.0	71.2

[a] Condition: 10 mM sodium phosphate buffer pH 6.0-8.0, 100 mM NaCl, [PNA] = 1.0 μM and [DNA] = 1.0 μM

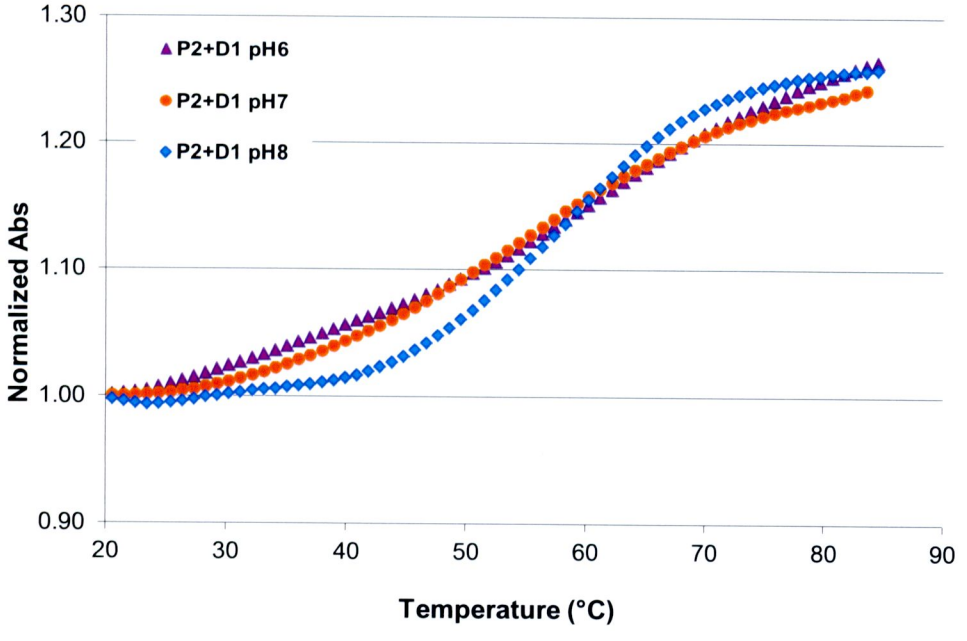

Figure 36 T_m curves of DNA (D1) with PNA (P2) hybrid at pH 6.0-8.0 Condition: 100 mM NaCl, [PNA] = 1.0 μM and [DNA] = 1.0 μM

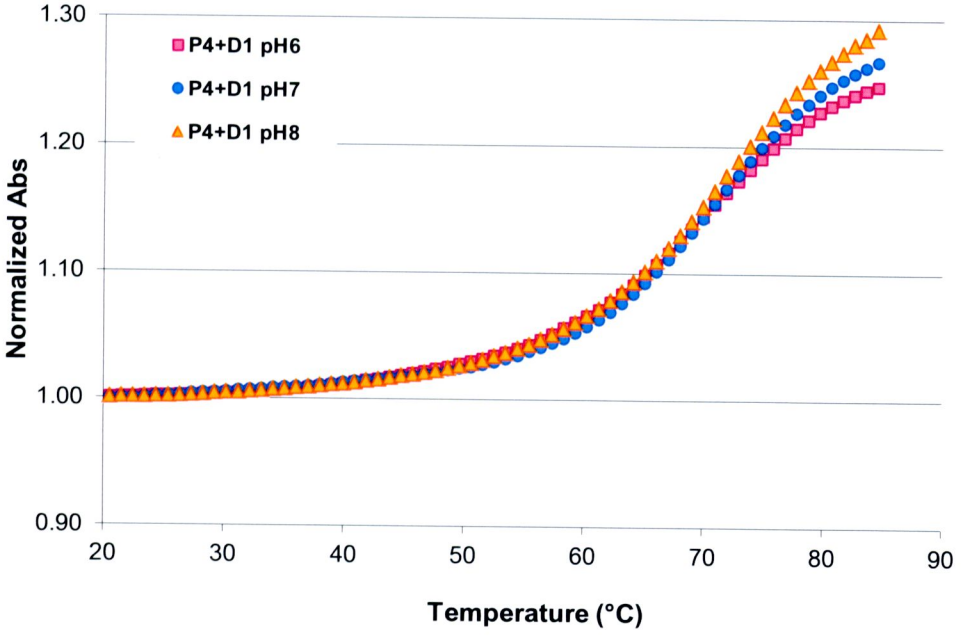

Figure 37 T_m **curves of DNA (D1) with PNA (P4) hybrid at pH 6.0-8.0 Condition: 100 mM NaCl, [PNA] = 1.0 μM and [DNA] = 1.0 μM**

The effect of ionic strength to PNA·DNA hybrid was also studied. Different concentration of NaCl had much effect on T_m of the fully modified *apc*PNA (**P2**) and its complementary DNA (**D1**) hybrids in a 1:1 mixture (Figure 38 and Table 7). In these experiments, the T_m value is decreased under higher salt concentration, this phenomenon is in opposite direction to that DNA·DNA hybrid but similar to Nielsen's PNA·DNA hybrid. It has been suggested that the counterion release upon helix formation rather than counterion uptake as in the case DNA·DNA [52]. This effect is much less pronounced in the PNA (**P4**) which was singly modified in the middle of the strand with APC spacer (Figure 39).

Table 7 T_m data of DNA (D1) with PNA (P2, P4) hybrid at [NaCl] 0-500 mM.

PNA	DNA sequence (5'→3')	[NaCl] (mM)	T_m (°C) [a]
P2	(D1) AAAAAAAAA	0	72.0
		100	55.5
		500	23.7
P4	(D1) AAAAAAAAA	0	76.7
		100	70.9
		500	66.0

[a] Condition: 10 mM sodium phosphate buffer pH 7.0, 0-500 mM NaCl, [PNA] = 1.0 μM and [DNA] = 1.0 μM

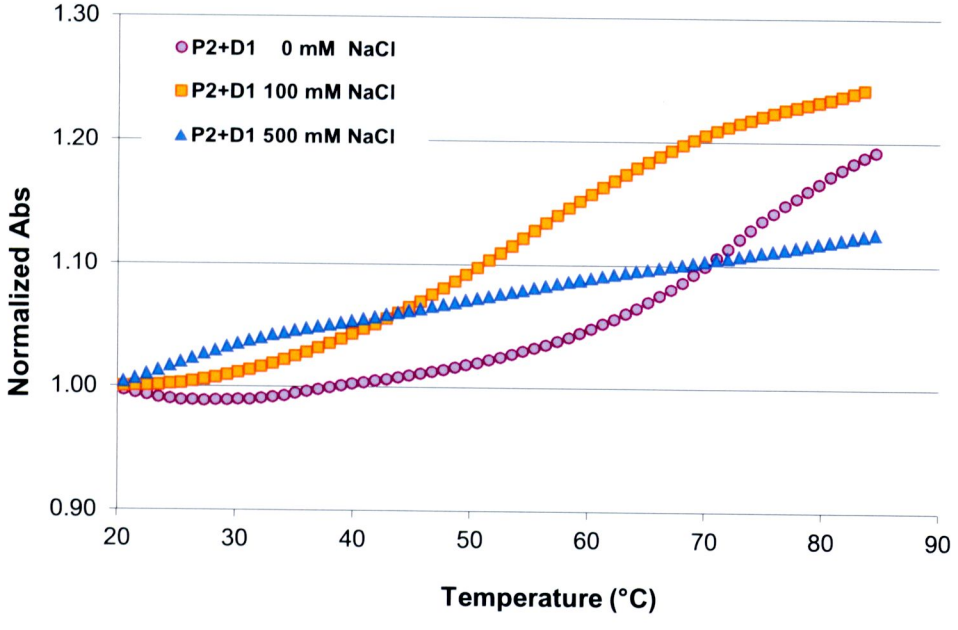

Figure 38 T_m curves of DNA·PNA (P2) hybrid at [NaCl] = 0, 100, 500 mM Condition: 10 mM sodium phosphate buffer pH 7.0, [PNA] = 1.0 μM and [DNA] = 1.0 μM

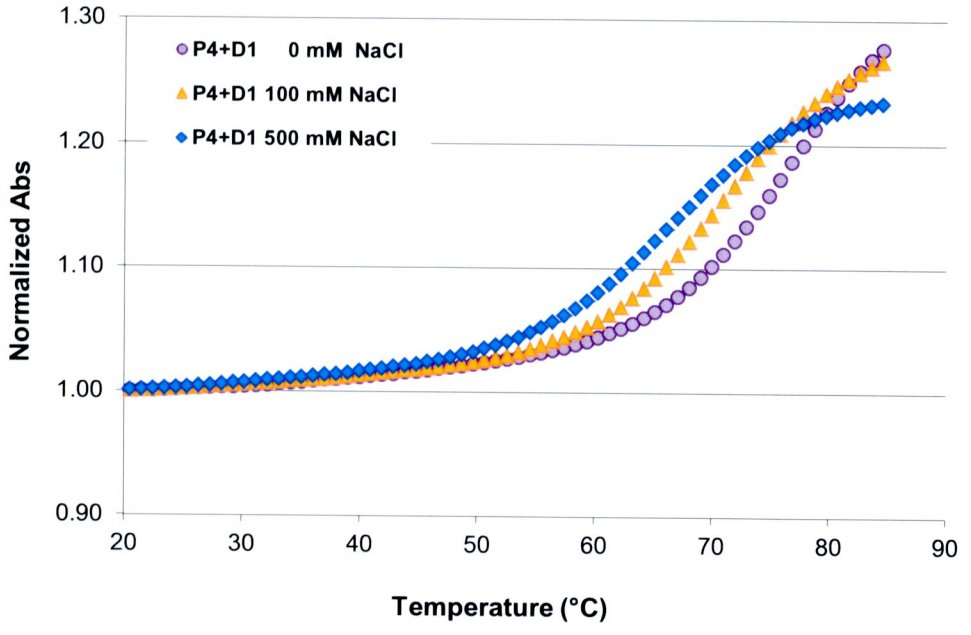

Figure 39 T_m curves of DNA·PNA (P4) hybrid at [NaCl] = 0, 100, 500 mM Condition: 10 mM sodium phosphate buffer pH 7.0, [PNA] = 1.0 μM and [DNA] = 1.0 μM

The result of studies showed the *apc*PNAs (**P2** and **P4**) can bind with complementary DNA with T_m only slightly lower than unmodified *acpc*PNA. The single modified in *apc*/*acpc*PNA (**P4**) could be used as a handle for incorporation of fluorophores such as pyrene in the middle of the PNA strand *via* the N^1 position of the APC spacer, which will be discussed in the next topic.

Application of fluorescent labeled PNA as a probe for DNA sequence analysis

The preliminary experiments of the *apc*/*acpc*PNA probes to use for DNA sequence analysis. Two fluorescent labeling groups, namely pyrenecarboxylyl and pyrenebutyryl have been successfully attached at ^1N of APC spacer of PNA oligomers using solid phase strategy. The pyrene fluorescent label was attached on the nitrogen atom in APC spacer of PNA **P7, P8, P9** and **P10** by deprotecting N^1-trifluoroacetyl group on the PNA oligomers followed by coupling with pyrenecarboxylic acid (Py) or pyrenebutyric acid (PyBu). All steps were carried out while the PNA was still attached

on the solid support. The T_m value of pyrene-labeled PNA (**P7-10**) with complementary DNA was dramatically decreased suggesting destabilization due to steric effects (Table 8). Fluorescence of the pyrene labeled PNA·DNA hybrid was detected by UV lamp and fluorescence spectrophotometer, which was carried out at 2.5 μM each of PNA probe (**P7-10**) and 3.0 μM of DNA in 10 mM phosphate buffer pH 7.0 (total volume 1000 μL). The fluorescence emission of the pyrenecarboxylic acid modified homothymine PNA (**P7**) exhibited an increase in the fluorescence intensity at 382 nm by ~3.6-fold upon hybridization with dA_9 (Figure 40). The some PNA gave barely noticeable change upon hybridization with a single mismatch DNA target (dA_4TA_4). Unfortunately, the mixed base sequence **P9** exhibited the fluorescence change that was considerably smaller (~1.3 fold) as shown in Figure 41. The fluorescence change of **P7** could be visualized by naked eyes under UV irradiation (Figure 42).

Table 8 T_m data of PNA (P7-P10) oligomers in this study.

PNA sequence (N→C) [a]		DNA sequence (5'→3')	Corrected T_m (°C) [b]	Δ T_m (°C) [c]
P7 TTTT(Py)TTTTT	**D1**	AAAAAAAAA	63.5	-
	D2	AAAATAAAA	26.8	36.7
P8 TTTT(PyBu)TTTTT	**D1**	AAAAAAAAA	60.3	-
	D2	AAAATAAAA	25.4	34.9
P9 GTAGA(Py)TCACT	**D3**	AGTGATCTAC	44.3	-
	D4	AGTGACCTAC	26.3	18.0
P10 GTAGA(PyBu)TCACT	**D3**	AGTGATCTAC	45.6	-
	D4	AGTGACCTAC	25.4	20.2

[a] T = (1*S*,2*S*)-ACPC-T; G = (1*S*,2*S*)-ACPC-G; C = (1*S*,2*S*)-ACPC-C; A = (1*S*,2*S*)-ACPC-A; T = (3*R*,4*S*)-APC-T; (Py) = pyrene-1-carbonyl modification; (PyBu) = 4-(pyrene-1-yl)butyryl modification

[b] Condition: **P7-P10** = 10 mM sodium phosphate buffer pH 7.0, [PNA] = 2.5 μM and [DNA] = 3.0 μM

[c] $\Delta T_m = T_m$(complementary) – T_m(mismatched) (same PNA, different DNA)

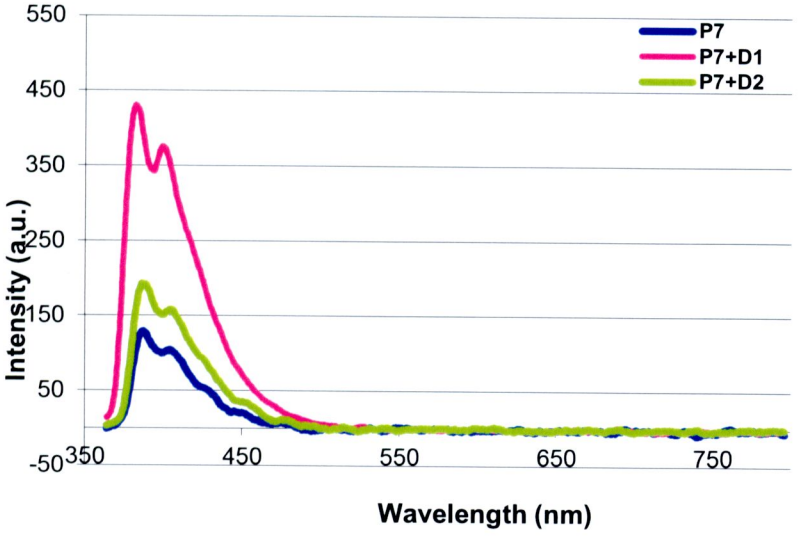

Figure 40 **Fluorescence spectra of pyrene-labeled *apc/acpc*PNA P7 (—), P7 + complementary DNA (—), P7 + single mismatch DNA (—). Conditions: 10 mM sodium phosphate buffer, pH 7.0, [PNA] = 2.5 μM and [DNA] = 3.0 μM, excitation wavelength = 345 nm.**

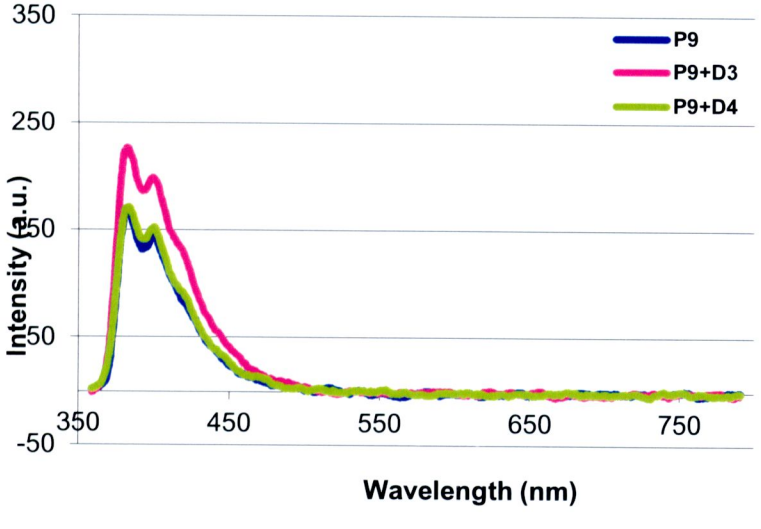

Figure 41 **Fluorescence spectra of pyrene-labeled *apc/acpc*PNA P9 (—), P9 + complementary DNA (—), P9 + single mismatch DNA (—). Conditions: 10 mM sodium phosphate buffer, pH 7.0, [PNA] = 2.5 μM and [DNA] = 3.0 μM, excitation wavelength = 345 nm.**

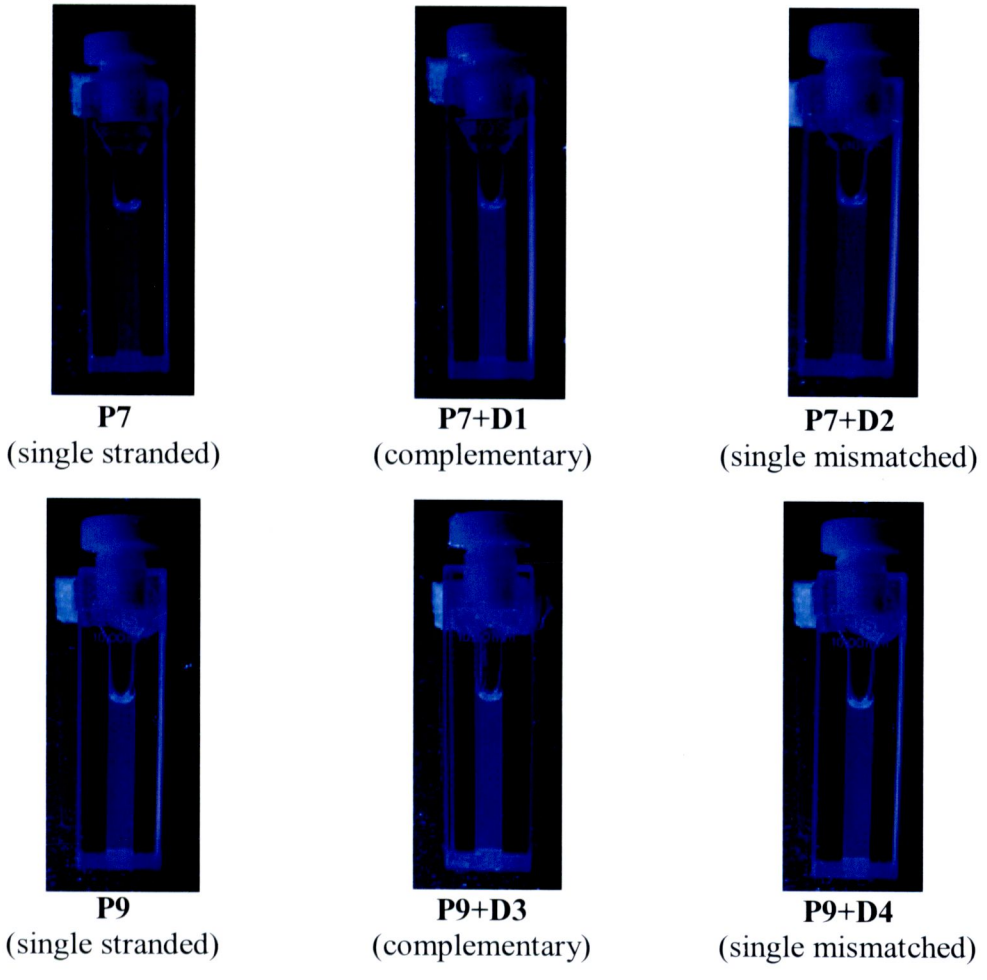

Figure 42 Photographs of pyrene-labeled P7 and P9 in the presence and absence of the DNA targets under UV light (365 nm). Conditions: 10 mM sodium phosphate buffer, pH 7.0, [PNA] = 2.5 μM and [DNA] = 3.0 μM

The pyrenebutyric acid modified homothymine PNA (**P8**) exhibited very a large enhancement of fluorescent intensity at 379 nm (over 70 folds) upon hybridization with dA_9. Only weak fluorescence enhancement was observed with a single mismatch DNA target (dA_4TA_4) (Figure 43). For the mixed base sequence **P10,** the fluorescence increase was considerably smaller (~4.8 fold) (Figure 44). However, the fluorescence is significantly higher compared to the single stranded **P10** and its hybrid with single mismatched DNA (Figure 45).

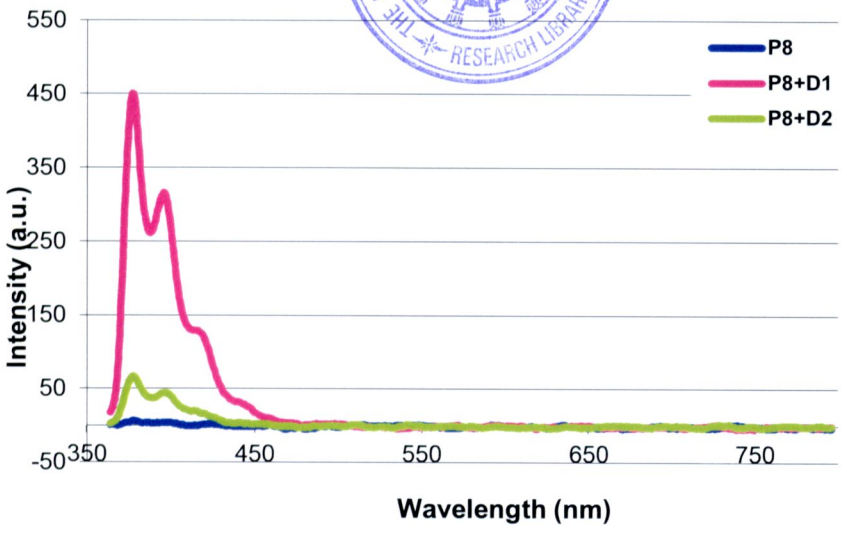

Figure 43 **Fluorescence spectra of pyrene-labeled *apc/acpc*PNA P8 (—), P8 + complementary DNA (—), P8 + single mismatch DNA (—). Conditions: 10 mM sodium phosphate buffer, pH 7.0, [PNA] = 2.5 μM and [DNA] = 3.0 μM, excitation wavelength = 345 nm.**

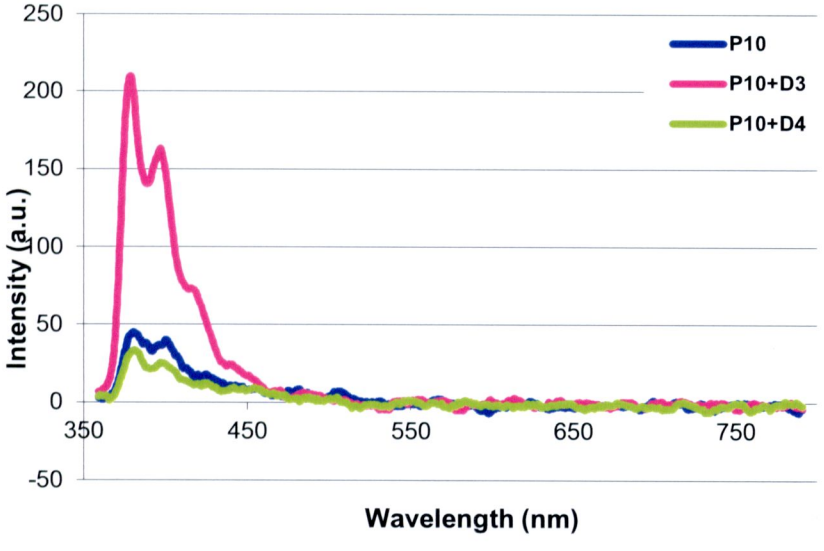

Figure 44 **Fluorescence spectra of pyrene-labeled *apc/acpc*PNA P10 (—), P10 + complementary DNA (—), P10 + single mismatch DNA (—). Conditions: 10 mM sodium phosphate buffer, pH 7.0, [PNA] = 2.5 μM and [DNA] = 3.0 μM, excitation wavelength = 345 nm.**

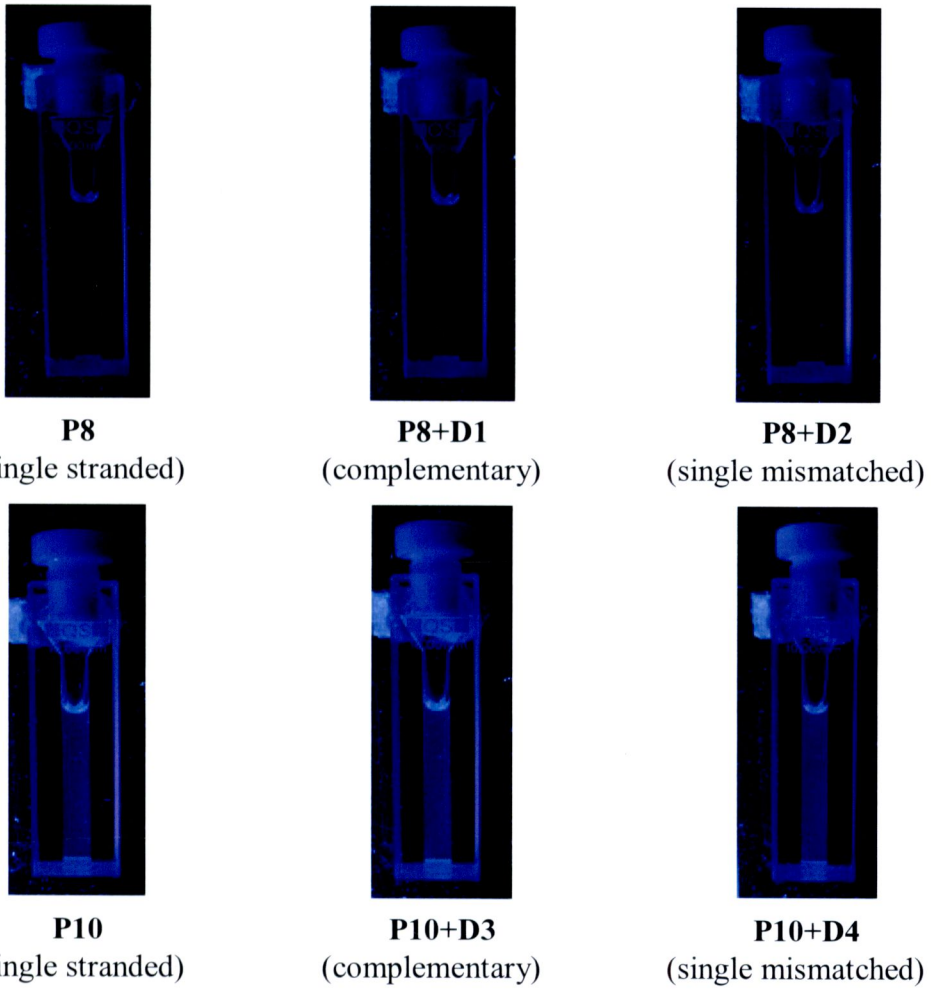

Figure 45 Photographs of pyrene-labeled P8 and P10 in the presence and absence of the DNA targets under UV light (365 nm). Conditions: 10 mM sodium phosphate buffer, pH 7.0, [PNA] = 2.5 μM and [DNA] = 3.0 μM

The singly modified apc/acpcPNA labeled with pyrenecarbonyl and pyrenebutyryl labels (**P7**, **P8**, **P9** and **P10**) have been successfully preliminary applicaton for DNA sequence analysis. These revealed that the pyrenebutyryl labels on *apc/acpc*PNA showed very high differentials of fluorescent intensity than pyrenebutyryl labels on *apc/acpc*PNA because distance between the pyrenebutyryl label and the nucleobase which acted as quencher so far by the side-chain of pyrenebutyryl group. From the results, the pyrene labeled *apc/acpc*PNA system showed a good potential to be used as a fluorescence probe which is sensitive to its

hybridization state and can readily distinguish between complementary and single-mismatched DNA targets, which can be useful for DNA sequence determination.

Table 9 Fluorescent intensity of the PNA (P7-P10) oligomers

PNA sequence (N→C) [a]		DNA sequence (5'→3')		Fluorescent intensity
P7	TTTT(Py)$\underline{T}$TTTT	**D1**	AAAAAAAAA	3.0 fold
		D2	AAAATAAAA	1.3 fold
P8	TTTT(PyBu)$\underline{T}$TTTT	**D1**	AAAAAAAAA	over 70 fold
		D2	AAAATAAAA	10.2 fold
P9	GTAGA(Py)$\underline{T}$CACT	**D3**	AGTGATCTAC	1.3 fold
		D4	AGTGACCTAC	1.0 fold
P10	GTAGA(PyBu)$\underline{T}$CACT	**D3**	AGTGATCTAC	4.8 fold
		D4	AGTGACCTAC	0.8 fold

[a] T = (1*S*,1*S*)-ACPC-T; G = (1*S*,1*S*)-ACPC-G; C = (1*S*,1*S*)-ACPC-C; A = (1*S*,2*S*)-ACPC-A; $\underline{T}$ = (3*R*,4*S*)-APC-T; (Py) = pyrene-1-carbonyl modification; (PyBu) = 4-(pyrene-1-yl)butyryl modification

[b] Condition: **P7-P10** = 10 mM sodium phosphate buffer pH 7.0, [PNA] = 2.5 μM and [DNA] = 3.0 μM

[c] Fluorescent intensity = Fluorescent intensity (single-strand *acpc*PNA) – Fluorescent intensity (double-strand *acpc*PNA with DNA) (same PNA, different DNA)